International Journal of Environmental Sciences
ISSN: 2229-7359
Vol. 11 No. 23s, 2025
https://theaspd.com/index.php

# Implications of Paleoweathering And Sediment Maturity in Geochemical Characterisation of Kalijhora Sandstones Exposed in The Extra-Peninsular Gondwana Basin, Darjeeling District, West Bengal, India

**Dr. Ranjeeta Kar[1], Dr. Hrishikesh Baruah[2], Dr. Sarat Phukan[3]**
[1]Department of Geology, Sibsagar University, Joysagar, Sivasagar-785665, Assam, India
[2]K.C. Das Commerce College, Chatribari, Guwahati-781008, Assam, India
[3]Department of Geological Sciences, Gauhati University, Jalukbari, Guwahati-781014, Assam, India
Corresponding Author: Dr. Ranjeeta Kar: rkar@sibsagaruniversity.ac.in
**ORCID id**: 0000-0003-3462-0948

***ABSTRACT***
*This study examines specific geochemical attributes of extra-peninsular Kalijhora Gondwana sandstones from Darjeeling District, West Bengal, aiming to elucidate their weathering intensity, climatic conditions, and sediment maturity based on major oxide data. The Chemical Maturity Index (CMI) rises as quartz becomes more concentrated (60.57%-78.99%), replacing less resistant minerals through processes of weathering, transportation, and recycling. Elevated Al2O3 content (average 11.48%) results from finer particles and K-feldspar alteration, while K2O/Na2O ratios suggest K-feldspar transformation into Illite. Palaeo-weathering indices like high CIA (61.56%-77.55%), CIW (40.78%-92.80%), and PIA (32.59%-91.02%) values reveal intense weathering of source rocks. The Weathering Index of Parker (WIP) values (1275.37-3771.49), Vogel's Index (V) values (1.05-6.24), and Silica-Titania Index (STI) values (72.94-93.01) indicate advanced weathering stages. The Index of Compositional Variability (ICV) values (0.62-6.95) suggest compositionally mature sediments. Hydraulic sorting effects indicate a recycled sedimentary source, with provenance discrimination diagrams highlighting deposition under active continental collision and compression. The findings align with the regional geological evolution of the Gondwana basin, indicating mature sediments from recycled sources deposited in a tectonically active setting influenced by post-collision uplift. Regionally, the Gondwana basin deepened northwards during the Gondwana period, with palaeo-current directions oriented towards north, suggesting a source in the Precambrian metamorphic terrain south of the basin. Significant detrital contributions likely came from the Eastern Ghats Supergroup and possibly the Transantarctic Mountains. This study highlights the complex interplay of weathering, transportation, and sediment recycling in shaping the geochemical characteristics of Kalijhora Gondwana sandstones.*
***Keywords***: *Kalijhora Gondwana sandstones, geochemistry, Palaeo-weathering indices, Hydraulic sorting, recycled sedimentary source.*

## 1. INTRODUCTION

The chemical composition of clastic sedimentary rocks is influenced by various factors, including the original rock composition, weathering processes, climatic conditions during weathering, transportation mechanisms, the depositional environment of the basin, and post-depositional alterations (Hayashi et al. 1997, Singh et al. 2016). Consequently, geochemical analysis of clastic sediments provides valuable insights into their provenance, chemical weathering, hydraulic sorting, and sediment abrasion. Numerous studies have explored these aspects, elucidating the origin of both ancient and modern siliciclastic sediments (Dickinson and Suczek 1979, Nesbit and Young, 1982, 1984, 1996, Bhatia 1983, Roser and Korsch 1988, Condie 1993, Mclennan et. al. 1993, Cullers 2000). Additionally, the decomposition of unstable minerals is often assessed using the Chemical Index of Weathering (CIW) and the Chemical Index of Alteration (CIA) (Nesbit and Young 1982, Harnois 1988). The CIA index particularly predicts the transformation of feldspar minerals, which are prevalent rock-forming minerals in the Earth's crust (Mclennan et. al. 1993). Several other weathering indices, such as the $Al_2O_3/Fe_2O_3$, $SiO_2/Fe_2O_3$, $SiO_2/Al_2O_3$, and $K_2O/Al_2O_3$ ratios, Weathering Index of Parker (WIP), Vogel's Index (V), Plagioclase Index of Alteration (PIA), Silica-Titania Index (STI), the Index of Compositional Variability (ICV), and the $Al_2O_3$–($CaO$+$Na_2O$)–$K_2O$ (A–CN–K) ternary plots, are frequently used to interpret the maturity and provenance of rocks. Hence, clastic sediment geochemistry is exhaustively utilised for determination of facets ranging from chemical maturity, sediment recycling to relating sediments with their plate tectonic settings.

The present venture aims to ascertain certain relevant geochemical attributes of the Kalijhora Gondwana sandstones situated in the extra-peninsular Kalijhora Basin in the Darjeeling District of West Bengal, (Fig. 1) taking into consideration the variation of major oxides to work out the inter-relation between these concentrates. The data has been vigorously subjected to critical evaluations pertaining to the behaviour of these concentrates under impact of tectonic setup of the provenance, rates of weathering, climatic conditions, and environment of deposition.

**2. Geology of the study area**

The Gondwana rocks exposed in and around Kalijhora area (Fig. 1), locally known as the Rishi Group, (Basu, 2013) forms a part of the extra-peninsular Kalijhora Gondwana basin located within the fold and thrust belts of Darjeeling- Sikkim Himalayas. These Late Palaeozoic Gondwana rocks aligned in a roughly ENE-WSW to WNW-ESE trend are sandwiched between Siwalik rocks lying to the south and Precambrian Dalings exposed to the north (Table 1).

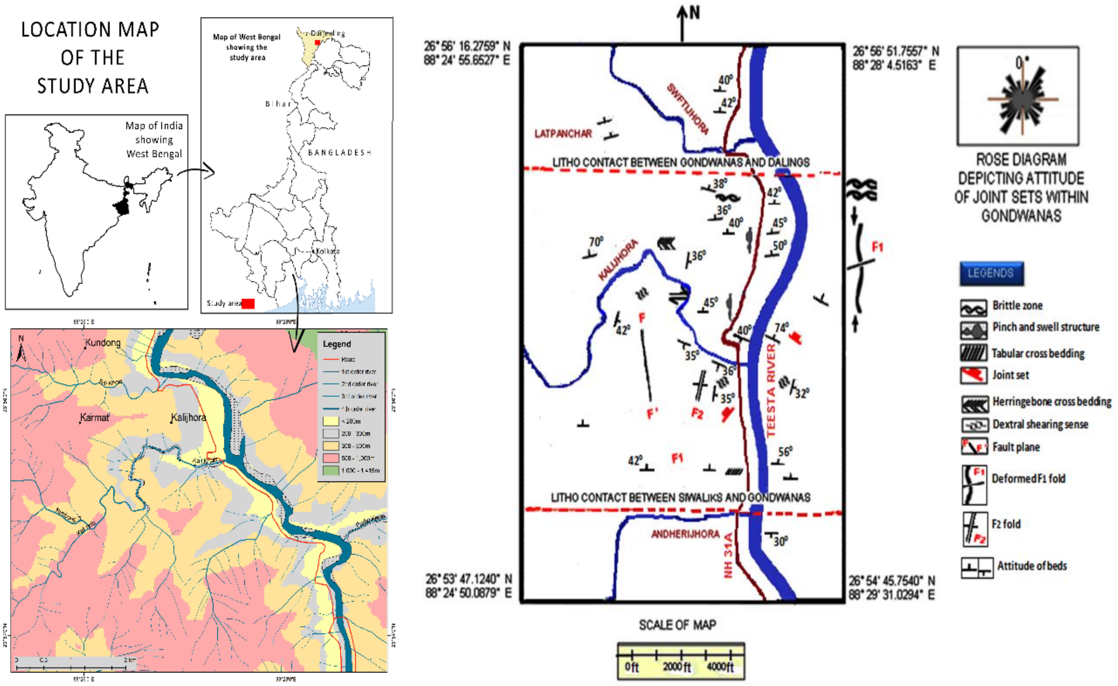


**Fig. 1** Location map of Kalijhora in West Bengal of India after Kar et al. 2022


**Fig. 2a**


**Fig. 2b**


**Fig. 2c**

**Fig. 2a** Coal is intermixed with sandstone and display an anthracitic look demonstrating thrusting effect; locality: Right bank of Kalijhora river; **Fig. 2b** Hard blocky medium to fine sandstone along right bank of Kalijhora river bed; **Fig. 2c** Alternation of sandstone and coal.

**Table 1** Synthesised lithostratigraphy of Kalijhora area (HFT: Himalayan Frontal Thrust; SKT: South Kalijhora Thrust; MBT: Main Boundary Thrust; DT: Daling Thrust; after Kar et al. 2020)

| AGE | GROUP | LITHOTYPES |
|---|---|---|
| Recent | | Alluvium |

~ ~ ~ ~ ~ ~ ~ ~ ~ ~ ~ ~ ~ ~ ~ ~ ~ Thrusted (HFT) ~ ~ ~ ~ ~ ~ ~ ~ ~ ~ ~ ~ ~ ~ ~

Tertiary Siwalik Medium grained sandstone, carbonaceous shale intercalated with sandy shale, silt, minor marl and pebbly sandstones, conglomerate: Repetitive sequence

~ ~ ~ ~ ~ ~ ~ ~ ~ ~ ~ ~ ~ ~ ~ ~ ~ ~ ~ ~ Thrusted (SKT) ~ ~ ~ ~ ~ ~ ~ ~ ~ ~ ~ ~ ~ ~ ~ ~ ~

Fine to medi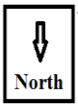

dstone, sandy shale, shale, minor coal, pebbly sandstones, conglomerate

~ ~ ~ ~ ~ ~ ~ ~ ~ ~ ~ ~ ~ ~ ~ ~ ~ ~ Thrusted (MBT) ~ ~ ~ ~ ~ ~ ~ ~ ~ ~ ~ ~ ~ ~ ~ ~

Fine to medium grained buff-coloured sandstones

Permo-Carboniferous Gondwana / Rishi Grey coloured sandstones intercalated with slaty shale, carbonaceous shale, and coal; minor gritty sandstones; few sandstones exude a calcareous look

Grey to dark grey recrystallised sandstone

~ ~ ~ ~ ~ ~ ~ ~ ~ ~ ~ ~ ~ ~ ~ ~ ~ Thrusted (DT) ~ ~ ~ ~ ~ ~ ~, ~ ~ ~ ~ ~ ~ ~ ~ ~ ~

Precambrian Daling Massive quartzites

Intercalations of foliated quartzites and phyllites

The lithostratigraphic column of Kalijhora is seen to be largely arenaceous (Kar et al. 2019) whereby dominantly medium grained Gondwana sandstones (Fig. 2b) occur as varieties of dark grey sandstones in the southernmost sequence, designated as the $Ar_1$ unit; grey middle unit, named as $Ar_2$; and buff coloured, little bit recrystallised variety, distinguished as the northernmost $Ar_3$ unit. The grey sandstone varieties of the middle unit are exposed along the Kalijhora river bed and it hosts variable calcareous components. The sandstones here depict warped, discontinuous bedding planes and presence of cross joints and curviplanar joint planes; and are interlayered with sandy shale, carbonaceous shale, and coal displaying an anthracitic look (Fig. 2a, 2c) under impact of thrusting in proximity to the zone of MBT. Kalijhora area shows conspicuous imprints of Himalayan geodynamism and is devoid of fossils. A larger antiform like feature can be worked out in the region across the Kalijhora River that has an east-west axial planar trend and a fold axis which is moderately westerly plunging (Kar et al. 2020), and has been witnessed to exude signatures of dextral shear sense, exhibited by the ductile coal and carbonaceous shale layers in the form of Z-type crenulations (Baruah et. al., 2018).

## 3. METHODOLOGY

Geochemical analyses of 20 representative samples from the study area were considered to evaluate their chemical constitution regarding major oxides, trace and rare earth elements at Wadia Institute of Himalayan Geology, Dehradun, India. For the present study, major oxides $SiO_2$, $TiO_2$, $Al_2O_3$, $Fe_2O_3$, MnO, MgO, CaO, $Na_2O$, $K_2O$, and P2O5 weight % were determined in samples vide XRF technique (S8 Tiger from Bruker-AXS, Germany). The major oxides mentioned above were employed to analyze and interpret various geochemical plots, aiming to determine the provenance and tectonic setting of the sandstones. $SiO_2/Al_2O_3$–$Na_2O/K_2O$ diagram, A–CN–K diagram, and R, WIP, V, CIW, CIA, PIA, STI and ICV values were employed to assess the impacts of source weathering, climatic conditions, sediment maturity, and hydraulic sorting processes (Nesbit and Young 1982, 1984, Harnois 1988, Ohta 2004, Ohta and Arai 2007).

## 4. Geochemical findings and discussions

### 4.1 Relationship among Major Oxides and significant ratios

The percentages of major oxides from bulk representative samples of Kalijhora sandstones are presented in Table 2. Overall, the mean element abundances reflect the mineralogical characteristics of the Kalijhora sandstones. The decreasing trend in elemental proportions is as follows: $SiO_2 > Al_2O_3 > CaO > Fe_2O_3 > K_2O > MgO > Na_2O > TiO_2 > P_2O_5 > MnO$. The Kalijhora Gondwana sandstones exhibit a high $SiO_2$ concentration, ranging from 60.57% to 78.99 wt%, with an average of 70.61 wt%. It is noteworthy that $SiO_2$ has an average abundance of 66% in sandstones derived from the upper continental crust (Taylor and McLennan 1985). Variations in major element geochemistry are illustrated using Harker diagrams. These variations are analyzed in two groups: (i) in relation to $SiO_2$ and (ii) variations between other elements. For the Kalijhora sandstones, considering $SiO_2$ as a common factor, positive correlations are observed between $SiO_2$ and $Al_2O_3$, $K_2O$, and $Na_2O$, while negative correlations are observed with $Fe_2O_3$, MnO, CaO, MgO, and $P_2O_5$ (Fig. 3a). This trend is likely due to the dominance of free silica in the form of quartz, as well as contributions from aluminosilicates like feldspar and mica.

The presence of finer grain populations or the alteration of K-feldspars to clay minerals and the leaching of mica likely contribute to the relatively high $Al_2O_3$ content (average value of 11.48%). To determine the distribution patterns of $Al_2O_3$ with other oxides, plots of $Al_2O_3$ versus $Na_2O$, $SiO_2$, $K_2O$, $TiO_2$, $Fe_2O_3$, MgO, $P_2O_5$, CaO, and MnO were constructed (Fig. 3b). The plot of $Al_2O_3$ versus $Fe_2O_3$ shows a slight positive correlation. Moderate to strong positive correlations of $Na_2O$, $K_2O$, and TiO2 with $Al_2O_3$ suggest that the clastic sediments contain a modest amount of clay in that population (McLennan et al., 1983), indicating an association with phyllosilicates. This implies a probable source of input and suggests a significant impact of hydraulic sorting mechanisms (Haque and Roy 2020). In contrast, correlations of MgO, $P_2$O5, CaO, and MnO with $Al_2O_3$ display a low to moderate negative trend, indicating different sources.

The lower average $TiO_2$ content (0.44 wt%) suggests that the source rocks in the study area are more evolved (felsic). Additionally, the lower average $P_2$O5 content (0.15 wt%) indicates a lesser presence of accessory mineral phases such as apatite and monazite.

Table 3 presents various features of major oxide inter-relationships and ratios, analyzed in depth to understand rock chemistry, provenance, climatic conditions, and tectonic setting based on the work of Bhatia (1983), Suttner and Dutta (1986), and LeMaitre (1976). In sandstone analysis, key discriminating parameters include the $Al_2$O3/$SiO_2$ ratio, $Fe_2O_3$ + MgO %, $TiO_2$ %, $K_2O/Na_2O$, and $Al_2$O3/(CaO + $Na_2O$) ratios (cf. Bhatia 1983).

Titanite ($TiO_2$) is present in low percentages but remains persistently common even at such low concentrations. The $TiO_2$ concentration ranges from 0.27 to 0.70 wt%, with an average value of 0.44%. Possible sources of $TiO_2$ include metamorphosed argillaceous rocks, acidic igneous rocks (as detrital rutile and ilmenite), or pre-existing sedimentary rocks. $TiO_2$ is also commonly found in ferromagnesian minerals like biotite, amphibole, pyroxene, and olivine (Sawyer 1986). It is widely recognized that titanium is a very stable mineral phase, relatively immobile during weathering (Nesbitt 1979), and is characteristic of sediments that have experienced prolonged sub-aerial weathering. $TiO_2$ indicates a continental geochemical setting, with its content decreasing as the distance from land increases (Reineck and Singh 1980).

In this study, the low Mn/Fe ratio of 0.03 suggests a shallow water environment. A positive correlation between $K_2O$ and $Al_2$O3, with an average molar K/Al ratio of 0.20 (Table 3), suggests that K-bearing minerals significantly influence the distribution of aluminium. This correlation indicates that the abundance of these minerals is primarily controlled by the content of clay minerals (McLennan et al. 1983, Nath et al. 2000, Osae et al. 2006, Jin et al. 2006).

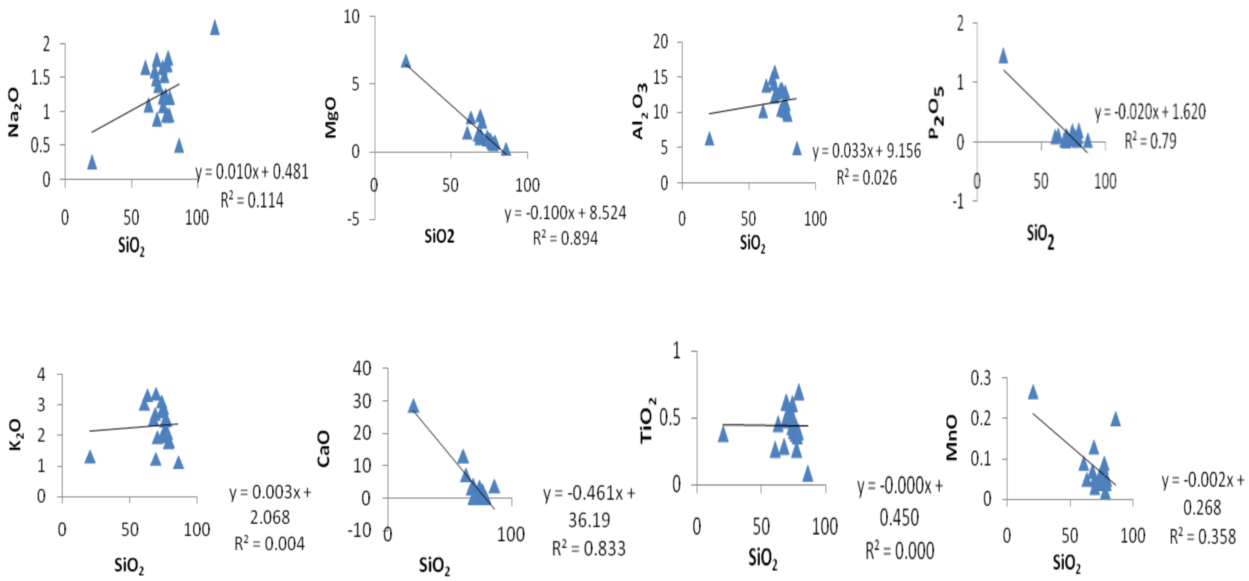


**Fig. 3a** Harkar variation diagrams between $SiO_2$ and other major oxides of Kalijhora sandstones

International Journal of Environmental Sciences
ISSN: 2229-7359
Vol. 11 No. 23s, 2025
https://theaspd.com/index.php

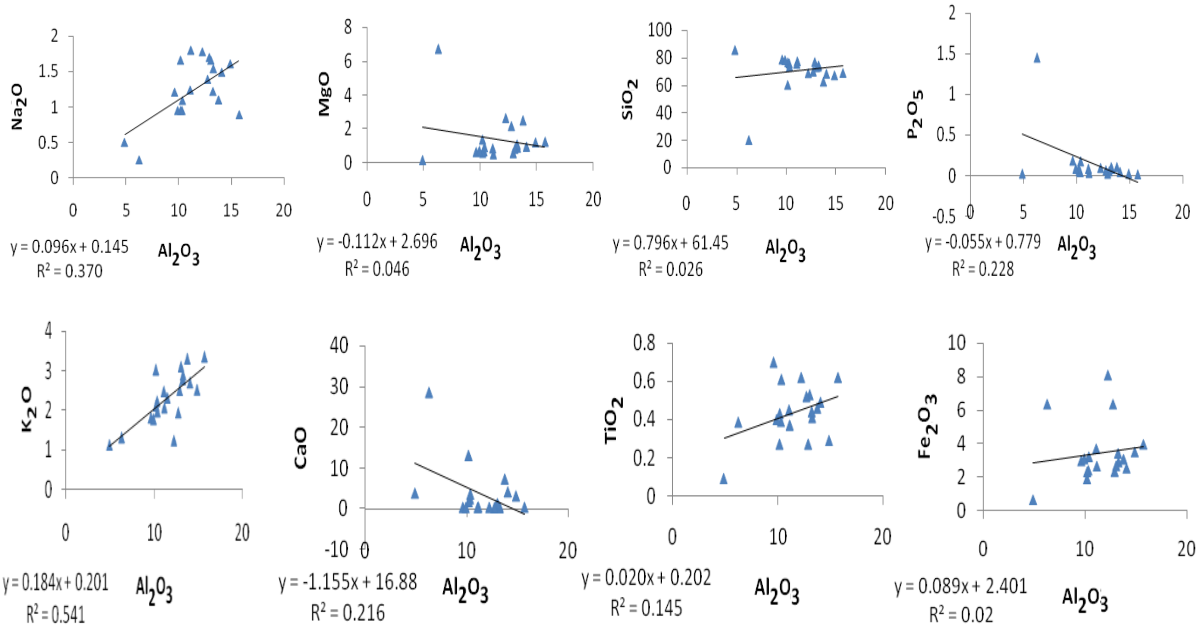


**Fig. 3b** Variation of $Al_2O_3$ with other major oxides of Kalijhora sandstones

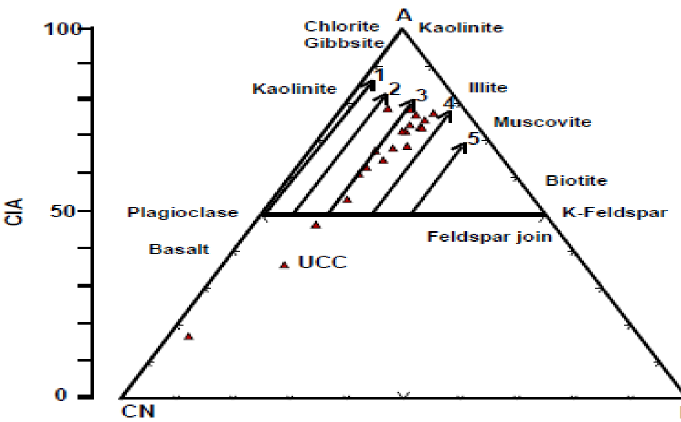


**Fig. 4** $Al_2O_3$-$CaO+Na_2O$-$K_2O$ ternary diagram (Nesbitt and Young 1984). Arrows 1-5 represent the weathering trends of gabbro, tonalite, granodiorite, adamellite and granite respectively.

**Table 2** Major oxides (in wt. %) of the Gondwana sandstones of Kalijhora area

| Sample | $Na_2O$ % | MgO % | $Al_2O_3$ % | $SiO_2$ % | $P_2O_5$ % | $K_2O$ % | CaO % | $TiO_2$ % | MnO % | $Fe_2O_3$ % | LOI % | Total % |
|---|---|---|---|---|---|---|---|---|---|---|---|---|
| RKH 1 | 0.95 | 0.73 | 10.31 | 76.27 | 0.05 | 2.23 | 2.43 | 0.39 | 0.08 | 2.44 | 2.72 | 98.6 |
| RKH 2 | 0.95 | 0.63 | 10.19 | 76.95 | 0.06 | 2.12 | 1.73 | 0.43 | 0.09 | 2.35 | 2.59 | 98.09 |
| RKH 3 | 0.5 | 0.2 | 4.87 | 85.99 | 0.03 | 1.12 | 3.8 | 0.09 | 0.2 | 0.69 | 3.15 | 100.64 |
| RKH 4 | 0.89 | 1.28 | 15.72 | 69.3 | 0.02 | 3.36 | 0.33 | 0.62 | 0.03 | 3.97 | 3.79 | 99.31 |
| RKH 5 | 1.21 | 0.68 | 9.61 | 78.99 | 0.19 | 1.81 | 0.31 | 0.7 | 0.05 | 2.99 | 1.81 | 98.35 |
| RKH 6 | 1.54 | 0.94 | 13.27 | 74.82 | 0.09 | 2.9 | 0.31 | 0.41 | 0.06 | 2.92 | 1.94 | 99.2 |
| RKH 7 | 1.22 | 1.12 | 13.23 | 73.64 | 0.11 | 2.79 | 0.27 | 0.44 | 0.04 | 3.44 | 2.29 | 98.59 |

| | | | | | | | | | | | | |
|---|---|---|---|---|---|---|---|---|---|---|---|---|
| **RKH 8** | **1.66** | **1.4** | **10.17** | **60.57** | **0.09** | **3.03** | **13.11** | **0.27** | **0.09** | **1.93** | **8.5** | **100.82** |
| **RKH 9** | **1.1** | **2.53** | **13.76** | **62.95** | **0.11** | **3.31** | **7.25** | **0.46** | **0.05** | **3.09** | **6.29** | **100.9** |
| **RKH 10** | **1.09** | **0.97** | **10.35** | **73.94** | **0.18** | **1.97** | **3.55** | **0.61** | **0.06** | **3.24** | **4.02** | **99.98** |
| **RKH 11** | **1.7** | **0.62** | **12.89** | **77.21** | **0.03** | **2.51** | **0.69** | **0.27** | **0.04** | **2.37** | **2.58** | **100.91** |
| **RKH 12** | **1.49** | **0.99** | **14.06** | **68.67** | **0.05** | **2.7** | **4.14** | **0.49** | **0.13** | **2.56** | **4.8** | **100.08** |
| **RKH 13** | **1.61** | **1.24** | **14.87** | **67.51** | **0.03** | **2.52** | **3.12** | **0.29** | **0.07** | **3.52** | **4.33** | **99.11** |
| **RKH 14** | **1.66** | **0.88** | **13.04** | **73.48** | **0.06** | **3.11** | **1.22** | **0.53** | **0.06** | **2.7** | **3.44** | **100.18** |
| **RKH 15** | **0.251** | **6.72** | **6.26** | **20.28** | **1.45** | **1.31** | **28.62** | **0.386** | **0.267** | **6.35** | **30.32** | **102.22** |
| **RKH 16** | **1.8** | **0.55** | **11.14** | **77.74** | **0.04** | **2.07** | **0.35** | **0.37** | **0.02** | **2.68** | **2.15** | **98.91** |
| **RKH 17** | **1.39** | **2.2** | **12.73** | **70.3** | **0.07** | **1.94** | **0.17** | **0.52** | **0.04** | **6.35** | **4.48** | **100.19** |
| **RKH 18** | **1.78** | **2.67** | **12.23** | **69.11** | **0.1** | **1.23** | **0.31** | **0.62** | **0.05** | **8.07** | **3.23** | **99.4** |
| **RKH 19** | **1.24** | **0.89** | **11.08** | **75.82** | **0.09** | **2.48** | **0.27** | **0.45** | **0.05** | **3.71** | **2.51** | **98.59** |
| **RKH 20** | **0.95** | **0.75** | **9.9** | **78.58** | **0.09** | **1.77** | **0.26** | **0.4** | **0.04** | **3.12** | **2.34** | **98.2** |
| **Avg** | **1.24905** | **1.4** | **11.484** | **70.606** | **0.1471** | **2.314** | **3.612** | **0.4373** | **0.0759** | **3.4245** | **4.864** | **99.613** |

**Table 3** Selected major oxide ratios of Gondwana sandstones of Kalijhora area

| Major element ratio | | | | | | | | | | | | | | | | | | | | | |
|---|---|---|---|---|---|---|---|---|---|---|---|---|---|---|---|---|---|---|---|---|---|
| Ratio | RKH1 | RKH2 | RKH3 | RKH4 | RKH5 | RKH6 | RKH7 | RKH8 | RKH9 | RKH10 | RKH11 | RKH12 | RKH13 | RKH14 | RKH15 | RKH16 | RKH17 | RKH18 | RKH19 | RKH20 | AVG. |
| $Fe_2O_3 + MgO$ | 3.17 | 2.98 | 0.89 | 5.25 | 3.67 | 3.86 | 4.56 | 3.33 | 5.62 | 4.21 | 2.99 | 3.55 | 4.76 | 3.58 | 13.07 | 3.23 | 8.55 | 10.74 | 4.6 | 3.87 | 4.82 |
| $Al_2O_3 / SiO_2$ | 0.14 | 0.13 | 0.06 | 0.23 | 0.12 | 0.18 | 0.18 | 0.17 | 0.22 | 0.14 | 0.17 | 0.21 | 0.22 | 0.18 | 0.31 | 0.14 | 0.18 | 0.18 | 0.15 | 0.13 | 0.17 |
| Na2O/K2O | 0.43 | 0.45 | 0.45 | 0.26 | 0.67 | 0.53 | 0.44 | 0.55 | 0.33 | 0.55 | 0.68 | 0.55 | 0.64 | 0.53 | 0.19 | 0.87 | 0.72 | 1.45 | 0.5 | 0.54 | 0.57 |
| $K_2O / Na_2O$ | 2.44 | 2.23 | 2.24 | 3.78 | 1.5 | 1.88 | 2.29 | 1.83 | 3.01 | 1.81 | 1.48 | 1.81 | 1.57 | 1.87 | 5.22 | 1.15 | 1.4 | 0.69 | 2 | 1.86 | 2.1 |
| $Al_2O_3 / (CaO + Na_2O)$ | 3.05 | 3.8 | 1.13 | 12.89 | 6.32 | 7.17 | 8.88 | 0.69 | 1.65 | 3.18 | 5.39 | 2.5 | 3.14 | 4.53 | 0.22 | 5.18 | 8.16 | 5.85 | 7.34 | 8.18 | 4.96 |
| $\log (Na_2O / K_2O)$ | -0.37 | -0.35 | -0.35 | -0.58 | -0.17 | -0.27 | -0.36 | -0.26 | -0.48 | -0.26 | -0.17 | -0.26 | -0.19 | -0.27 | -0.72 | -0.06 | -0.15 | 0.16 | -0.3 | -0.27 | -0.28 |
| $\log(Fe_2O_3 / K_2O)$ | 0.04 | 0.04 | -0.21 | 0.07 | 0.22 | 0 | 0.09 | -0.2 | -0.03 | 0.22 | -0.03 | -0.02 | 0.15 | -0.06 | 0.69 | 0.11 | 0.51 | 0.82 | 0.17 | 0.25 | 0.14 |
| $\log(SiO_2 / Al_2O_3)$ | 0.87 | 0.88 | 1.25 | 0.64 | 0.91 | 0.75 | 0.75 | 0.77 | 0.66 | 0.85 | 0.78 | 0.69 | 0.66 | 0.75 | 0.51 | 0.84 | 0.74 | 0.75 | 0.84 | 0.88 | 0.79 |
| $Al_2O_3 / Na_2O$ | 10.85 | 10.73 | 9.74 | 17.66 | 7.94 | 8.62 | 10.84 | 6.13 | 12.51 | 9.5 | 7.58 | 9.44 | 9.24 | 7.86 | 24.94 | 6.19 | 9.16 | 6.87 | 8.94 | 10.42 | 10.26 |
| $TiO_2 / Al_2O_3$ | 0.04 | 0.04 | 0.02 | 0.04 | 0.73 | 0.03 | 0.03 | 0.03 | 0.03 | 0.06 | 0.02 | 0.04 | 0.02 | 0.04 | 0.06 | 0.03 | 0.04 | 0.05 | 0.04 | 0.04 | 0.07 |
| $MnO / Fe_2O_3$ | 0.03 | 0.04 | 0.29 | 0.01 | 0.02 | 0.02 | 0.01 | 0.05 | 0.02 | 0.02 | 0.02 | 0.05 | 0.02 | 0.02 | 0.04 | 0.01 | 0.01 | 0.01 | 0.01 | 0.01 | 0.03 |
| $Al_2O_3 + K_2O + Na_2O$ | 13.49 | 13.26 | 6.49 | 19.97 | 12.63 | 17.71 | 17.24 | 14.86 | 18.17 | 13.41 | 17.1 | 18.25 | 19 | 17.81 | 7.82 | 15.01 | 16.06 | 15.24 | 14.8 | 12.62 | 15.05 |
| $SiO_2 / Al_2O_3$ | 7.4 | 7.55 | 17.66 | 4.41 | 8.22 | 5.64 | 5.57 | 5.96 | 4.57 | 7.14 | 5.99 | 4.88 | 4.54 | 5.63 | 3.24 | 6.98 | 5.52 | 5.65 | 6.84 | 7.63 | 6.55 |
| log(K2O/Na2O) | 0.37 | 0.35 | 0.35 | 0.58 | 0.17 | 0.27 | 0.36 | 0.26 | 0.48 | 0.26 | 0.17 | 0.26 | 0.19 | 0.27 | 0.72 | 0.06 | 0.14 | -0.16 | 0.3 | 0.27 | 0.28 |
| Al2O3/TiO2 | 26.44 | 23.7 | 54.11 | 23.35 | 13.73 | 32.37 | 30.07 | 37.67 | 29.91 | 16.97 | 47.74 | 28.69 | 51.28 | 24.6 | 16.22 | 30.11 | 24.48 | 19.73 | 24.62 | 24.75 | 29.03 |
| CaO+Na2O | 3.38 | 2.68 | 4.3 | 1.22 | 1.52 | 1.85 | 1.49 | 14.77 | 8.35 | 4.64 | 2.39 | 5.63 | 4.73 | 2.88 | 28.87 | 2.15 | 1.56 | 2.09 | 1.51 | 1.21 | 4.86 |
| Avg. | 0.22 | 0.21 | 0.23 | 0.21 | 0.19 | 0.22 | 0.21 | 0.3 | 0.24 | 0.19 | 0.19 | 0.19 | 0.17 | 0.24 | 0.21 | 0.19 | 0.15 | 0.1 | 0.22 | 0.18 | 0.2 |

### 4.2 Palaeoweathering inputs

Mineral chemistry, the intensity and duration of weathering, and climatic conditions are key factors influencing mineral alteration during chemical weathering. In the upper crust, one significant weathering process is the breakdown of feldspars and the formation of clay minerals. This feldspar degradation, a highly sensitive indicator of chemical weathering, leads to increased mobility of elements such as potassium, sodium, and calcium, which migrate into clay minerals and the soil profile (Taylor and McLennan 1985, Nesbitt et al. 1980). Additionally, chemical weathering of rocks results in the depletion of alkalis and alkaline earth metals, with a concurrent preferential enrichment of $Al_2O_3$ (Cingolani et al. 2003). Consequently, the residual substances in the soil and sediments can serve as a sensitive index of weathering intensity (Nesbitt et al. 1997).

In sandstone geochemistry, several chemical indices are used to assess the degree and nature of weathering processes. These indices help to understand the chemical alterations that the sandstones have undergone due to weathering, which in turn provide insights into the paleoclimate, diagenetic history, and provenance of the sedimentary rocks. The values of various indices for Kalijhora sandstones have been displayed in Table 4 and deductions have been made based on Table 5.

**4.2.1 Ruxton Ratio (R)**

It is a simple weathering index that uses the ratio of silica ($SiO_2$) to alumina ($Al_2O_3$):

$R= SiO_2/ Al_2O_3$

Weathering Intensity: Lower values of the Ruxton Ratio indicate more intense weathering, as alumina is more resistant to chemical weathering compared to silica (Ruxton 1968).

Mineral Stability: A low Ruxton Ratio suggests the relative enrichment of alumina-rich minerals (e.g., clays) due to the removal of silica (Ruxton 1968).

Paleoclimate: It can be used as an indicator of past climatic conditions, where a low ratio might suggest a warm and humid climate conducive to intense weathering (Ruxton 1968).

The R values for the Kalijhora sandstones range from 3.24 to 17.66, with an average of 6.55 (Table 4), indicating a high intensity of chemical weathering in the source areas. Thus, palaeoclimate condition can be deduced to be a hot and humid one which is similar to the petrographic finding (Kar et. al., 2020).

**4.2.2 Weathering Index of Parker (WIP)**

The Weathering Index of Parker (WIP) focuses on the mobility of major cations and the progression of weathering (Parkar 1970, Harnois 1988). It is calculated using the proportions of mobile and less mobile elements:

$WIP=[(2Na_2O/0.35) +(MgO/0.9) +(2K_2O/0.25) +(CaO/0.7)] \times 100$

Element Mobility: Reflects the degree to which mobile elements (Na, Mg, K, Ca) have been leached from the rock (Parkar 1970).

Weathering Progression: Lower WIP values indicate more advanced weathering stages (Parkar 1970).

Soil Formation: Provides insights into the processes of soil formation and mineral stability during weathering (Parkar 1970).

The WIP values for the Kalijhora sandstones range from 1275.37 to 3771.49, with an average of 2898.84 (Table 4), indicating more advanced weathering stages.

**4.2.3 Vogel's Index (V)**

Vogel's Index is another measure of weathering intensity, typically involving ratios of less mobile to more mobile elements. It reflects mineral stability and broader geochemical trends during weathering (Vogt 1927, Roaldset 1972).

Common formulation involves elements such as Al, Fe, Mg, and others, depending on specific studies. It is calculated as follows:

$V=(Al_2O_3+K_2O)\ (MgO+CaO+Na_2O)$

Mineral Stability: Indicates the stability of various minerals during weathering, with lower values often indicating greater weathering intensity (Vogt 1927).

Geochemical Trends: Helps identify trends in the chemical alteration of rocks and soils (Vogt 1927).

Weathering Profile: Assists in constructing weathering profiles and understanding element redistribution (Vogt 1927).

The V values for the Kalijhora sandstones range from 1.05 to 6,24, with an average of 3.85 (Table 4), indicating greater weathering intensity.

**4.2.4 Silica-Titania Index (STI)**

The Silica-Titania Index (STI) indicates the degree of silica leaching and overall weathering intensity (de Jayawardena and Izawa 1994). It is calculated as:

$STI=[(SiO_2/TiO_2)/ \{(SiO_2/ TiO_2)/ + (SiO_2/Al_2O_3) +( Al_2O_3/ TiO_2)\}] *100$

Silica Retention: High STI values indicate a higher retention of silica relative to titanium, suggesting less intense weathering.
Weathering Intensity: Lower STI values are associated with more intense weathering, where silica has been leached out significantly.
Source Rock Composition: Provides clues about the composition of the source rock and the degree of chemical alteration it has experienced.
The STI values for the Kalijhora sandstones range from 72.94 to 93.01, with an average of 82.86 (Table 4), indicating a high intensity of chemical weathering in the source areas (Price and Velbel 2003).
**4.2.5 The Chemical Index of Alteration (CIA)** is a calculated metric used to determine the extent of weathering and its impact on sedimentary rocks in the source region of the derived sediments (Nesbitt and Young 1982). The CIA value is determined using the formula:
CIA = $[Al_2O_3 / (Al_2O_3 + CaO\ sil. + Na_2O + K_2O)] \times 100$
where CaO sil. represents CaO associated with silicate phases. In this study, after subtracting $P_2O5$ (wt%) from the total CaO (wt%) to account for the apatite contribution, the average CaO value was found to be higher than the average $Na_2O$ value. This suggests a higher amount of calcite and/or dolomite in the samples, as indicated by petrographic data. Consequently, following the correction method by McLennan (1993) as cited in Shao JingQing and Yang ShouYe (2012) and Malick and Ishiga (2016), CaO sil. was considered equivalent to $Na_2O$. CIA values for fresh to completely weathered rocks range from 50 to 100, with the latter consisting entirely of secondary minerals. Therefore, the CIA is a reliable indicator of palaeo-weathering conditions, reflecting the ratio of primary minerals to secondary products in sedimentary rocks and monitoring the progressive weathering of feldspars to clay minerals (Fedo et al. 1995, Armstrong-Altrin et al. 2004). The CIA values for the sandstones range from 61.56 to 77.55%, with an average of 70.61% (Table 4), indicating a high intensity of chemical weathering in the source areas. Mineralogical changes that modify the initial composition of sediments and sedimentary rocks can be triggered by K-metasomatism, leading to potassium enrichment, which is a significant aspect of geochemical studies (Nesbitt and Young 1989, Condie 1993, Fedo et al. 1997). In the current study, petrographic data indicate a low presence of K-feldspars. Consequently, a $K_2O/Na_2O$ ratio greater than 1 suggests $K_2O$ enrichment, possibly due to the transformation of kaolinite into illite through reactions with potassium-bearing pore waters (Fedo et al. 1995), a phenomenon also observed under SEM.
**4.2.6 Chemical Index of Weathering (CIW)** proposed by Harnois (1988) and the **Plagioclase Index of Alteration (PIA)** introduced by Fedo et al. (1995) are both reliable indicators of the extent of weathering in the source area of sediments, complementing the previously discussed Chemical Index of Alteration (CIA). CIW and PIA can be worked as follows:
CIW = $100[Al_2O_3/ (Al_2O_3 + CaO + Na_2O)]$
PIA = $100[(Al_2O_3 - K_2O) / (Al_2O_3 + CaO + Na_2O - K_2O)]$
The concept of the Chemical Index of Weathering (CIW) is similar to the Chemical Index of Alteration (CIA), with the primary difference being the exclusion of K2O from the CIW calculation. Additionally, the CIW does not consider $Al_2O_3$ associated with K-feldspar. The Plagioclase Index of Alteration (PIA) is typically employed to monitor plagioclase weathering and can serve as an alternative to the CIW, given that plagioclase is abundant in silicate rocks and dissolves quickly. The CIW values for the Kalijhora sandstones range from 40.78% to 92.80%, with an average of 70.26%, while the PIA values range from 32.59% to 91.02%, averaging 65.36% (Table 4).
By analyzing all these indices collectively, geologists can infer the extent and nature of weathering, the stability of various minerals, and the past climatic conditions that influenced the sandstone formations. This comprehensive understanding is crucial for reconstructing the geochemical history of sedimentary environments. Hence in the present case, it is found that the values for CIA, PIA, and CIW exceed 60% and this finding suggests moderate to high weathering either at the source or during transport prior to deposition (Fedo et al. 1995).
**Table 4** Palaeoweathering indices calculated for Kalijhora Sandstones

| Sample | R | WIP | V | CIA | CIW | PIA | STI | ICV |
|---|---|---|---|---|---|---|---|---|
| RKH1 | 7.40 | 2543.68 | 4.77 | 71.40 | 75.31 | 70.506 | 85.25 | 0.86 |
| RKH2 | 7.55 | 2444.57 | 4.87 | 71.71 | 79.18 | 75.07 | 85.13 | 0.77 |
| RKH3 | 17.66 | 1275.37 | 4.99 | 69.67 | 53.11 | 46.584 | 93.01 | 1.34 |
| RKH4 | 4.41 | 3465.94 | 6.24 | 75.36 | 92.8 | 91.016 | 78.97 | 0.63 |

| | | | | | | | | |
|---|---|---|---|---|---|---|---|---|
| RKH5 | 8.22 | 2387.84 | 3.68 | 69.44 | 86.34 | 83.691 | 83.72 | 0.73 |
| RKH6 | 5.64 | 3524.44 | 4.02 | 68.94 | 87.76 | 84.861 | 82.76 | 0.65 |
| RKH7 | 5.57 | 3227.87 | 4.50 | 71.67 | 89.88 | 87.51 | 82.45 | 0.67 |
| RKH8 | 5.96 | 3765.27 | 2.80 | 61.56 | 40.78 | 32.588 | 83.72 | 2.09 |
| RKH9 | 4.57 | 3714.83 | 3.61 | 71.41 | 62.23 | 55.585 | 79.87 | 1.26 |
| RKH10 | 7.14 | 2462.35 | 3.91 | 71.38 | 69.05 | 64.363 | 83.41 | 1.05 |
| RKH11 | 5.99 | 3291.17 | 3.83 | 68.56 | 84.36 | 81.284 | 84.18 | 0.62 |
| RKH12 | 4.88 | 3334.29 | 4.22 | 71.23 | 71.41 | 66.863 | 80.67 | 0.85 |
| RKH13 | 4.54 | 3303.78 | 3.90 | 72.15 | 75.87 | 72.307 | 80.66 | 0.81 |
| RKH14 | 5.63 | 3771.49 | 3.85 | 66.97 | 81.91 | 77.518 | 82.09 | 0.74 |
| RKH15 | 3.24 | 1973.24 | 1.05 | 77.55 | 17.82 | 14.636 | 72.94 | 6.95 |
| RKH16 | 6.98 | 3002.83 | 3.18 | 66.27 | 83.82 | 80.838 | 85.00 | 0.67 |
| RKH17 | 5.52 | 2789.30 | 2.95 | 72.95 | 89.08 | 87.368 | 81.84 | 0.95 |
| RKH18 | 5.65 | 2552.10 | 2.16 | 71.86 | 85.41 | 84.034 | 81.46 | 1.15 |
| RKH19 | 6.84 | 2968.60 | 4.02 | 69.08 | 88.01 | 85.064 | 84.26 | 0.78 |
| RKH20 | 7.63 | 2177.90 | 4.40 | 72.96 | 89.11 | 87.045 | 85.73 | 0.70 |
| Avg | 6.55 | 2898.84 | 3.85 | 70.61 | 70.26 | 65.355 | 82.86 | 1.21 |

**Table 5** Deductions drawn from weathering Indices (based on Price and Velbel 2003)

| Index | Formula | Optimum fresh value | Optimum weathered value |
|---|---|---|---|
| R | >10 | 0 | No |
| WIP | >100 | 0 | Yes |
| V | <1 | Infinite | No |
| CIA | ≤50 | 100 | No |
| CIW | ≤50 | 100 | No |
| PIA | ≤50 | 100 | No |
| STI | >90 | 0 | No |

### 4.3 Sediment Maturity

The index compositional variation (ICV) is a useful metric for assessing the original characteristics and maturity of sediments, as well as the climatic conditions that prevailed during their formation (Cox et. al 1995). Minerals that exhibit high weathering intensity show the highest ICV trends, while more stable minerals, which undergo less weathering, display lower ICV values. Specifically, clay minerals in the montmorillonite group show a greater decrease in ICV compared to those in the kaolinite group (Cox et. al 1995). Moreover, sediments that are more mature and originate from tectonically stable or cratonic environments typically have low ICV values (less than 1.0). In contrast, first-cycle immature sediments found in tectonically active settings tend to have higher ICV values (greater than 1.0). For the analyzed samples, the ICV values of sandstone vary from 6.95 to 0.62, with an average value of 1.21 (Table 4). These ICV values indicate compositionally mature sediments and their deposition in a tectonically stable environment. ICV is mathematically calculated as:

$ICV = (Fe_2O_3 + K_2O + Na_2O + CaO + MgO + MnO)/Al_2O_3$

In the present venture, $K_2O/Na_2O$ ratio ranges from 0.69% to 5.22% with an average of 2.10%. $K_2O$ and $Na_2O$ percentages and their ratios ($K_2O/ Na_2O >1$) represent relatively smaller amount of Na-rich plagioclase in the sandstones. The high values hint at derivation from granitic source (Potter 1978). This inference is also confirmed by the associated clay mineral content, as illite and kaolinite have been known to bear genesis from weathering horizons or soils developed on silicic rocks. This ratio has been concluded to increase with sedimentary maturation as feldspars and other less resistant fractions are labile during diagenesis (Crook 1974, Roser and Korsch 1986). Thus, in the Kalijhora sandstones, these ratios indicate moderate to high maturity of sediments (Wronkiewicz and Condie 1987) and this can also be compared with the ICV values which again increase with the maturity of rocks (Bhatia 1983, Haque and Roy 2020).

The scatter plot of CIA against ICV for the samples under investigation (Fig. 5) displays matured samples which were derived from intensively weathered source rocks.

Furthermore, sediment recycling often impacts the $Al_2O_3/SiO_2$ ratio in siliciclastic rocks and serves as a measure of sediment maturity. The Kalijhora sandstones exhibit low $Al_2O_3$/ $SiO_2$ values, ranging from 0.14 to 0.23, with an average of 0.17, indicating a high quartz content. The high SiO2 percentage, averaging 70.61%, along with the $SiO_2$/ $Al_2O_3$ ratio, which spans from 3.24 to 17.66 and averages 6.55, provides insight into the chemical maturity index (CMI). This index increases as quartz becomes more concentrated through the weathering, transport, and recycling processes, replacing less durable minerals (Maynard et al. 1982, Roser and Korsch 1986). The low $K_2O$/ $Al_2O_3$ values, ranging from 0.15% to 0.24%, likely indicate sedimentary recycling or enhanced weathering in the source area. Furthermore, the $SiO_2/Al_2O_3$-$Na_2O/K_2O$ plot (Fig.6) shows the impact of hydraulic sorting and indicates that the sediments were originated primarily from a recycled sedimentary provenance (Ohta, 2004). The chemical maturity of these sandstones is also evident from the $TiO_2$/ $Al_2O_3$ ratio (Jenner et al. 1981), which varies from 0.02 to 0.73, with an average of 0.07.

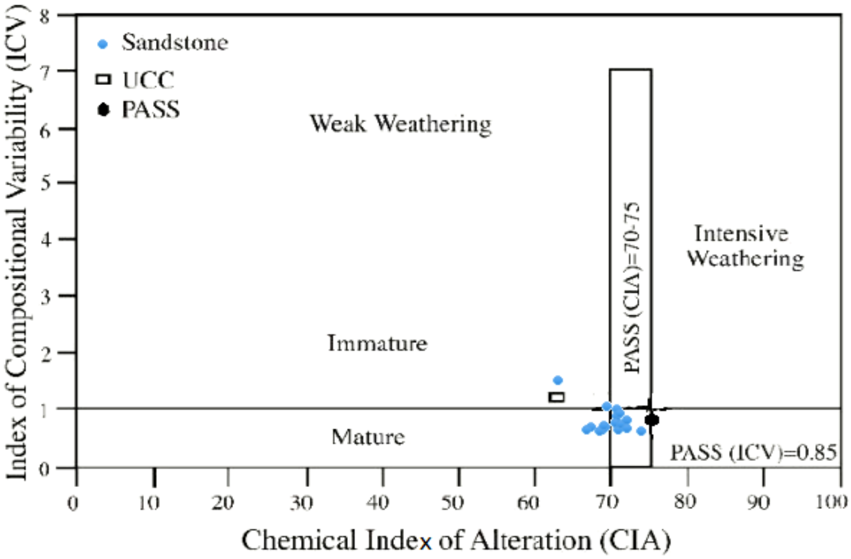


**Fig. 5** Binary plot of CIA vs ICV of Kalijhora sandstones

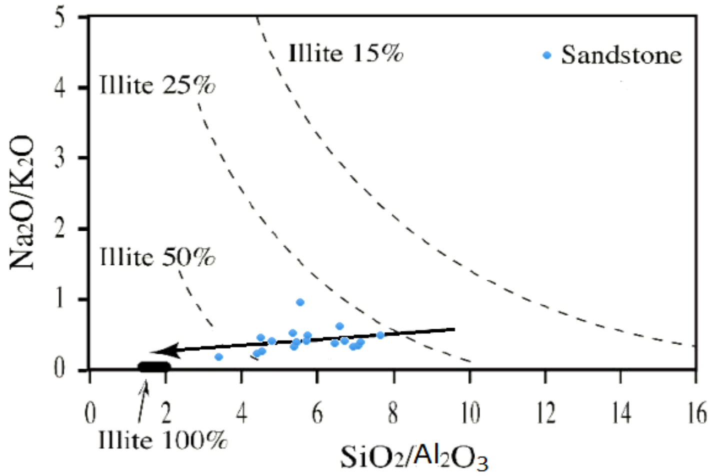


**Fig. 6** $SiO_2/Al_2O_3$-$Na_2O/K_2O$ plot of Kalijhora sandstones displaying the impact of hydraulic sorting (after Ohta 2004).

**5. Deductions and conclusion**

Based on the present geochemical studies of Kalijhora Gondwana sandstones, the following concluding observations may be drawn:

i. The analysis of major oxide data provides insights into the maturity of the sediments. The Chemical Maturity Index (CMI) rises as quartz becomes more concentrated, replacing less resistant minerals through processes of weathering, transportation, and recycling. The presence of finer particles or the alteration of K-feldspars into clay minerals, along with the leaching of mica, likely contributes to a relatively high $Al_2O_3$ content. $K_2O/Na_2O$ ratio greater than 1 suggests an enrichment of $K_2O$, possibly due to the transformation of Kaolinite into Illite through interactions with potassium-rich pore waters. Furthermore, the low $K_2O$/ $Al_2O_3$ values point to contributions from recycled sedimentary sources.

ii. The sediments originated from the upper continental crust, with the source rocks exhibiting a range of physico-chemical characteristics that led to differential erosion. Palaeo-weathering assessments, utilizing R, WIP, V, CIA, PIA, STI and CIW indices, reveal that the source rocks experienced moderate to intense weathering. Values for CIA, PIA, and CIW exceeding 60% suggest substantial weathering occurred either at the source or during the transportation phase prior to deposition.

iii. The $SiO_2/Al_2O_3$–$Na_2O/K_2O$ trend reflects hydraulic sorting effects, indicating that the sediments primarily originated from a recycled sedimentary source. The CIA, ICV, and $K_2O/Na_2O$ ratios suggest that the sediments exhibit moderate to high maturity, derived from both weakly and highly weathered source rocks. Tectonic provenance discrimination diagrams indicate that the sediments were predominantly deposited under the influence of active continental collision and compression. Mature sediments were delivered to the depositional basin following the uplift of source areas post-collision.

On a regional scale, the Gondwana basin in this part of the present-day Sikkim-Darjeeling Himalayan region deepened northwards towards Namchi in Sikkim (Basu, 2013), with palaeo-current directions also oriented northwards. Under these circumstances it is highly probable that anastomosing streams flowing from south along gentle palaeoslopes carried abundant mixed and suspended reworked sediments from southern low to medium grade metamorphic terrain like Eastern Ghats and Chotanagpur Plateau whereby the contributions of detritus from the denuded Precambrian Eastern Ghats Supergroup were very high (Baruah et al., 2018; Kar et al., 2022). Some contributions may also have been from distant sources located in the Trans-Antarctican Mountains (Tewari and Veevers, 1993). These streams flowed on large deltaic plains supporting lavishly vegetated swamps and marshes, eventually resulting in a fining upward sequence with presence of coal in a near shore fluvio-deltaic environment.

**Acknowledgements**

Ranjeeta Kar is thankful to Department of Science & Technology (DST), Govt. of India for providing the required financial assistance through the DST Inspire Fellowship (Ph.D. Programme). The authors are thankful to Wadia institute of Himalayan Geology, Dehradun for instrumentation facilities provided for sandstone geochemical analysis.

**REFERENCES**

1. Armstrong-Altrin, J.S. Lee, Y.I. Verma, S.P. & Ramasamy S. (2004). Geochemistry of Sandstones from the Upper Miocene Kundankulam Formation, Southern India: Implications for Provenance, Weathering, and Tectonic Setting. Journal of Sedimentary Research, 74, 285-297. https://doi.org/10.1306/082803740285.
2. Baruah, H., Kar, R.; Phukan, S.; Das, P.K.; Deka, M. & Dey, T. (2018) Sources and transport of the heavy minerals in some Gondwana basins of extra-pensular eastern India. The Jour. of the Indian Association of Sedimentologists, 35 (no.2), special volume dedicated to George Devries Klein, 59-81.
3. Basu, S.K. (2013). Geology of Sikkim state and Darjeeling district of West Bengal. Geological Society of India, Bangalore, 1st edition, xiv+256.
4. Bhatia, M.R. (1983). Plate tectonics and geochemical composition of sandstones. Jour. Geol., 91, 611-627.
5. Cingolani, C.A., Manassero, M. & Abre, P. (2003). Composition, Provenance and Tectonic Setting of Ordovician Siliciclastic Rocks in the San Rafael Block: Southern Extension of the Pre-Cordillera Crustal Fragment, Argentina. Jour. of South American Earth Sciences, 16, 91-106.
6. Condie, K.C. (1993). Chemical Composition and Evolution of Upper Continental Crust: Contrasting Results from Surface Samples and Shales. Chemical Geology, 104, 1-37.
7. Cox, R., Low, D. R. & Cullers, R. L. (1995). The influence of sediment recycling and basement composition on evolution of mudrock chemistry in the southwestern United States. Geochim. Cosmochim. Acta, 59 (14), 2919-2940. https://doi.org/10.1016/0016-7037(95)00185-9.
8. Crook, K.A.W. (1974). Lithogenesis and geotectonics: the significance of compositional variation in flysch arenites (graywackes). Soc. Econ. Paleontol. Min., Special Publication, 19, 304–310.
9. Cullers, R. L. (2000). The geochemistry of shales, siltstones, and sandstones of Pennsylvanian–Permian age, Colorado, USA: implications for provenance and metamorphic studies. Lithos, 51: 4937(99), 00063-8.
10. Dickinson, W.R. & Suczek, C.A. (1979). Plate tectonics and sandstone composition. Bull. Am. Assoc. Petrol. Geol., 63, 2164-2182.
11. Fedo, C.M., Nesbitt, H.W. & Young, G.M. (1995). Unraveling the effects of potassium metasomatism in sedimentary rocks and paleosols, with implications for weathering conditions and provenance. Geology, 23, 921–924.
12. Fedo, C.M., Young, G.M., Nesbitt, H.W. & Hanchar, J.M. (1997). Potassic and sodic metasomatism in the Southern Province of the Canadian Shield: evidence from the Palaeoproterozoic Serpent Formation, Huronian Supergroup, Canada. Precambrian Research, 84, 17-36.

13. Haque, Md. M. & Roy, M. K. (2020). Sandstone-Shale Geochemistry of Miocene Surma Group in Bandarban Anticline, SE Bangladesh: Implications for Provenance, Weathering, and Tectonic Setting. Earth Sciences, 9(1), 38-51. https://doi.org/10.11648/j.earth.20200901.15.
14. Harnois, L. (1988). The New Index, a New Chemical Index of Weathering. Sedimentary Geology, 55, 319-322.
15. Hayashi, K., Fujisawa, H., Holland, H. & Ohmoto, H. (1997). Geochemistry of ~1.9Ga sedimentary rock from northern Labrador Canada. Geochemica et cosmochimica Acta, 61 (19), 4115-4137. DOI: 10.1016/S0016-7037(97)00214-7.
16. Jason, R Price & Michael, A Velbel (2003). Chemical weathering indices applied to weathering profiles developed on heterogeneous felsic metamorphic parent rocks. Chemical Geology, 202 (Issues 3–4), 397-416. https://doi.org/10.1016/j.chemgeo.2002.11.001.
17. Jenner, G.A., Fryer B.J. &, Mclennan, S.M. (1981). Geochemistry of the Archean Yellowknife Supergroup. Geochimica et Cosmochimica Acta, 45, 1111-1129.
18. Jin, Z., Li F., Cao J., Wang S. & Yu J. (2006). Geochemistry of Daihai Lake sediments, Inner Mongolia, north China: Implications for provenance, sedimentary sorting and catchment weathering. Geomorphology, 80, 147-163.
19. Kar, R., Baruah, H. & Phukan, S. (2019). Signatures of Marine Influences in the Gondwana Sandstones of Kalijhora, Darjeeling district, West Bengal, India. Earth Sci. India, 12 (no.1), 24-37.
20. Kar, R., Phukan, S. & Baruah, H. (2020). Sedimentological evaluation of the coal bearing Gondwana sequence in and around Kalijhora, Darjeeling District, West Bengal, Ph.D. Thesis, University of Gauhati, http://hdl.handle.net/10603/290554.
21. Kar, R., Phukan, S. & Baruah, H. (2022). Organic Geochemical Assessment and Characterisation of Extra-Peninsular Gondwana Coal from Kalijhora Basin, Darjeeling District, West Bengal, India. Journal of the Geological Society of India, 98. 505-515. 10.1007/s12594-022-2008-z.
22. Lemaitre, R.W. (1976). The chemical variability of some common igneous rocks. Jour. Petrology, 17, 589-637.
23. Malick, B.M.L. & Shiga H. (2016). Geochemical Classification and Determination of Maturity Source Weathering in Beach Sands of Eastern San' in Coast, Tango Peninsula, and Wakasa Bay, Japan. Earth Science Research, 5 (1), 44-56.
24. Maynard, J.B., Valloni, R. & Yu, H.S. (1982). Composition of modern deep-sea sands from arc related basins. Trench-Forearc Geology: Sedimentation and tectonics on modern and ancient active plate margin, Geol. Soc. London Spec. Pub., 10, 551-651.
25. Mclennan, S.M., Taylor, S.R. & Eriksson, K.A. (1983). Geochemistry of Archean shales from the Pilbara Supergroup, Western Australia. Geochim Cosmochim Acta, 47, 1211-1222.
26. Mclennan, S.M., Hemming, S., Mcdaniel, D.K. & Hanson, G.N. (1993). Geochemical approaches to sedimentation, provenance, and tectonics. In Johnsson, M.J. and Basu, A. (Eds.), Processes Controlling the composition of Clastic Sediments, Special Paper (pp. 21–40). Geological Society of America.
27. Nath, B.N., Kunzendorf, H. & Pluger, W.L. (2000). Influence of provenance, weathering and sedimentary processes on the elemental ratio of the fine-grained fraction of the bed load sediments from the Vembanad Lake and the adjoining continental shelf, southwest Coast of India. Jour. Sed. Res., 70, 1081-1094.
28. Nesbitt, H.N. (1979). Mobility and fractionation of rare earth elements during weathering of a granodiorite. Nature, 279, 206–210.
29. Nesbitt, H.W., Fedo, C.M. & Young, G.M. (1997). Quartz and feldspar stability, steady and non-steady state weathering and petrogenesis of siliciclastic sands and muds. Jour. of Geology, 105, 173–191.
30. Nesbitt, H.W., Markovics, G. & Price, R.C. (1980). Chemical Processes affecting Alkalis and Alkali Earths during Continental Weathering. Geochimica et Cosmochimica Acta, 44, 1659-1666.
31. Nesbitt, H.W. & Young, G.M. (1982). Early Proterozoic climates and plate motions inferred from major element chemistry of lutites. Nature, 299, 715–717.
32. Nesbitt, H.W. & Young, G.M. (1984). Prediction of Some Weathering Trends of Plutonic and Volcanic Rocks Based on Thermodynamic and Kinetic Considerations. Geochimica et Cosmochimica Acta, 48, 1523-1534. http://dx.doi.org/10.1016/0016-7037(84)90408-3.
33. Nesbitt, H.W. & Young, G.M. (1989). Formation and diagenesis of weathering profiles. The Jour. of Geology, 97 (no.2), 129-147.
34. Nesbitt, H.W. & Young, G.M. (1996). Petrogenesis of sediments in the absence of chemical weathering: effects of abrasion and sorting on bulk composition and mineralogy. Sedimentology, 43, 341–358.
35. Ohta, T. (2004). Geochemistry of Jurassic to earliest Cretaceous deposits in the Nagato Basin, SW Japan: implication of factor analysis to sorting effects and provenance signatures. Sedimentary Geology, 171, 159–180. https://doi.org/10.1016/j.sedgeo.2004.05.014.
36. Ohta, T. & Arai H. (2007). Statistical empirical index of chemical weathering in igneous rocks: a new tool for evaluating the degree of weathering. Chemical Geology, 240, 280–297. https://doi.org/10.1016/j.chemgeo.2007.02.017.
37. Osae, S., Asiedu, D.K., Yakubo, B., Koebrel, C. & Dampare, S.B. (2006). Provenance and tectonic setting of Late Proterozoic Buem sandstones of southeastern Ghana: Evidence from geochemistry and detrital modes. Jour. African Earth Sci., 44, 85-96.
38. Parker, A. (1970). An Index of Weathering for Silicate Rocks. Geological Magazine, 107, 501-504. https://doi.org/10.1017/S0016756800058581.
39. Potter, P.E. (1978). Petrology and chemistry of modern big river sands. Jour. Geology, 86, 423-449.
40. Price, J.R. & Velbel, M.A. (2003). Chemical Geology, 202, 397-416. http://dx.doi.org/10.1016/j.chemgeo.2002.11.001.
41. Reineck, H.E. & Singh, I.B. (1980). Depositional Sedimentary Environments. Springer-Verlag, New York, 549 p.
42. Roaldset, E. (1972). Mineralogy and geochemistry of Quaternary clays in the Numedal Area, southern Norway. Norsk Geolisk Tidsskrift, 52, 335-369.
43. Roser, B.P. & Korsch, R.J. (1986). Determination of Tectonic Setting of Sandstone-Mudstone Suites Using SiO2 Content and K2O/Na2O Ratio. The Journal of Geology, 94, 635-650. https://doi.org/10.1086/629071.
44. Roser, B.P. & Korsch, R.J. (1988). Provenance signatures of sandstone-mudstone suites determined using discriminant function analysis of major-element data. Chemical Geology, 67, 119-139.

45. Ruxton, B.P. (1968). Measures of the Degree of Chemical Weathering of Rocks. Journal of Geology, 76, 518-527. https://doi.org/10.1086/627357.
46. Sawyer, E.W. (1986). The influence of source rock type, chemical weathering and sorting on the geochemistry of clastic sediments from the Quetico metasedimentary belt, Superior Province, Canada, Chem. Geol. 55, 77–95.
47. Shao, J. & Yang, S. (2012). Does chemical index of alteration (CIA) reflect silicate weathering and monsoonal climate in the Changjiang River basin? Chinrse Science Bulletin, 57 (10), 1178-1187.
48. Singh, A., Debajyoti, P., Sinha, R., Thomsen, K. J. & Gupta, S. (2016). Eochemistry of Buried River sediment from Ghaggar Plains NW India: multi-proxy records of variations in provenance, paleoclimate and paleovegetation patterns in the Late Quaternary. Palaeoecology, Palaeogeography Palaeoclimatology, 449. https://doi.org/10.1016/j.palaeo.2016.02.012.
49. Suttner, L.J. & Dutta, P.K. (1986). Alluvial Sandstone composition and Palaeoclimate Framework Mineralogy, Jour. Sed. Petrol., 56, 329-345.
50. Taylor, S.R. & Mclennan, S.M. (1985). The continental crust: its composition and evolution. Blackwell, London.
51. Tewari, R.C. & Veevers, J.J. (1993). Gondwana basins of India occupy the middle of a 7500 km sector of radial valleys and lobes in central-eastern Gondwanaland. Eighth intern. Gond. Symposium, Hobart, Australia, 507-512.
52. Vogt, T. (1927). Sulitjelmafeltets geologi og petrografi. Norges Geologiske Undersokelse, 121, 1-560. (In Norwegian, with English Abstract).
53. Wronkiewicz, D. J & Condie, K. C. (1987). Geochemistry of Archean shales from the Witwatersrand Supergroup, South Africa: source-area weathering and provenance. Geochim. Cosmochim. https://doi.org/10.1016/0016-7037(87)90293-6.